ELSEVIER

Journal of Nuclear Materials 271&272 (1999) 472–477

journal of nuclear materials

Influence of neutron irradiation on deformability and fracture micromechanisms of titanium α-alloys

O.A. Kozhevnikov *, E.V. Nesterova, V.V. Rybin, I.I. Yarmolovich

The State Research Centre CRISM 'Prometey', Spalernaya 49, 193167 St. Petersburg, Russian Federation

Abstract

The deformability and fracture appearance of neutron irradiated Ti–Zr alloy were investigated. It was shown that irradiation at 200–250°C resulted in a drastic decrease of uniform elongation. The material irradiated at 350°C and over was characterized by high deformability. The dimple ductile transgranular fracture was found to be typical for the examined material both in initial state and after the low temperature irradiation. Elements of ductile intergranular fracture were observed in the material after neutron irradiation at 400°C.

1. Introduction

The titanium α-alloys are characterized by a high specific strength, plasticity, corrosion resistance, low disposition to vacancy swelling, low (as compared with austenitic steels) disposition to be activated in neutron flux, small modulus of elasticity and small thermal expansion coefficient [1,2]. This unique combination of properties along with low atom number, high workability and good weldability allows the titanium alloys to be considered as future advantageous materials for fusion reactors. However, lack of experimental data on irradiation influence within a large range of temperatures and neutron fluences makes it difficult to study more carefully the possible use of these materials in assemblies and components of fusion reactors.

One of the most studied alloys from the point of radiation resistance is the alloy RK-20, which was specially designed for nuclear power engineering. This alloy is an equilibrium, binary, solid solution of 20 mass percent zirconium in hcp α-titanium (Table 1). This high-plastic material of medium strength is not practically disposed to ageing and has a high corrosion resistance in corrosive environments, including H_2 environment. The neutron influence on mechanical and corrosion properties including hydrogenation, is carefully studied in papers [3,4]. In this paper data are presented on TEM microstructures and fracture mechanisms of RK-20 alloy with respect to its irradiation hardening and embrittlement within a wide range of irradiation temperatures as compared with Ti–Al–V alloy.

2. Experimental procedure

Chemical composition and mechanical properties of examined materials in the initial (unirradiated) state are given in Table 1.

The neutron irradiation up to the dose 4×10^{25} n/m^2 (E > 0.5 MeV) was carried out in the active zone of research water–water WWR-M reactor. The irradiation at the temperatures below 100°C was carried out directly in the flux of the coolant (water). At the higher temperatures the samples were irrradiated in the hermetical experimental assemblies with a controlled heat gap. Temperature control was performed by thermocouples. The fast reactor BOR-60 was used to achieve the maximum neutron fluence $\sim 2 \times 10^{26}$ n/m^2 (E > 0.1 MeV).

Methods of transmission and scanning electron microscopy were used to study the microstructure and micrography of the fracture surface of RK-20 alloy in its initial state and after irradiation with neutron fluence 4×10^{24} n/m^2 at 200 ~ 250°C and 400°C. The features

* Corresponding author. Tel.: +7-812 2741227; fax: +7-812 2741707; e-mail: rybin@prometey2.spb.su

0022-3115/99/$ – see front matter
PII: S0022-3115(98)00803-4

Table 1
Chemical composition and mechanical properties of the alloys

Alloy	Chemical composition, wt%				Phase composition	Mechanical properties $T_{test} = 20°C$				
	Al	Zr	V	Ti		σ_u, MPa	$\sigma_{0.2}$, MPa	δ_t, %	δ_u, %	Ψ, %
RK-20	–	20	–	the rest	α	615	520	29.0	17.5	66.0
PT-3B	5.0	–	2.5	the rest	α + 3.5%β	725	650	10.0	6	24.0

of the defect structure evolution in the process of plastic deformation were studied on the samples strained after low temperature (200 ~ 250°C) irradiation at uniaxial tension with a rate 10^{-3} sec^{-1} up to $\varepsilon = 3.3\%$.

3. Experimental results

3.1. Characteristics of radiation resistance

Figs. 1 and 2 show the radiation dose characteristic curves of the yield strength, uniform and total relative elongation of RK-20 alloy. It is characteristic of these curves that they have a long incubation period during which the properties do not appreciably change. The duration of the incubation period depends on irradiation temperature, chemical and phase composition. In the same figures are shown the radiation dose curves characterizing strength and plasticity of a typical $\alpha + \beta$ alloy of Ti–Al–V system (β-phase content is up to 5%, (Table 1)). It is seen that this material has a short incubation fluence as compared with one-phase alloy RK-20 and possesses a higher disposition to irradiation hardening and embrittlement up to the dose 2×10^{24} n/m^2.

Figs. 3 and 4 show curves of the yield strength and uniform elongation of RK-20 alloy as a function of irradiation temperature. Irradiation at temperatures less than 250°C results in a large irradiation hardening and embrittlement of the studied material while a temperature increase up to more than 300°C almost transfers the alloy into the class of materials weakly disposed to irradiation embrittlement. The absence of drastic changes in local area reduction Ψ should also be noted as a characteristic feature of the RK-20 alloy radiation

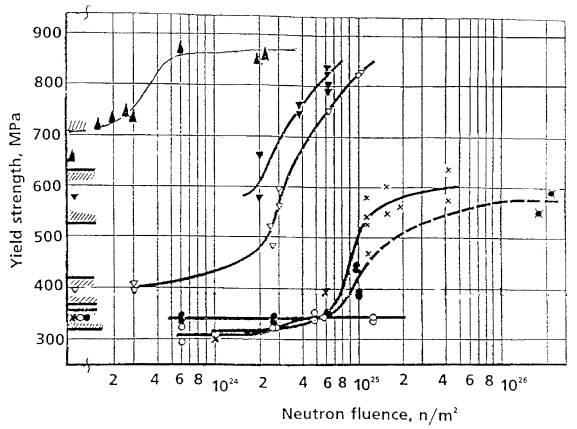

Fig. 1. Yield strength of RK-20 alloy as a function of neutron fluence (E ⩾ 0.5 MeV). Irradiation temperature, °C: ▼ – 50, ▽ – 230–250, × – 300, ● – 350–370, ○ – 400, – 360–380, reactor BOR-60 (E ⩾ 0.1 MeV), ▲ – 50, Ti–Al–V alloy. $T_{test} = T_{irr}$.

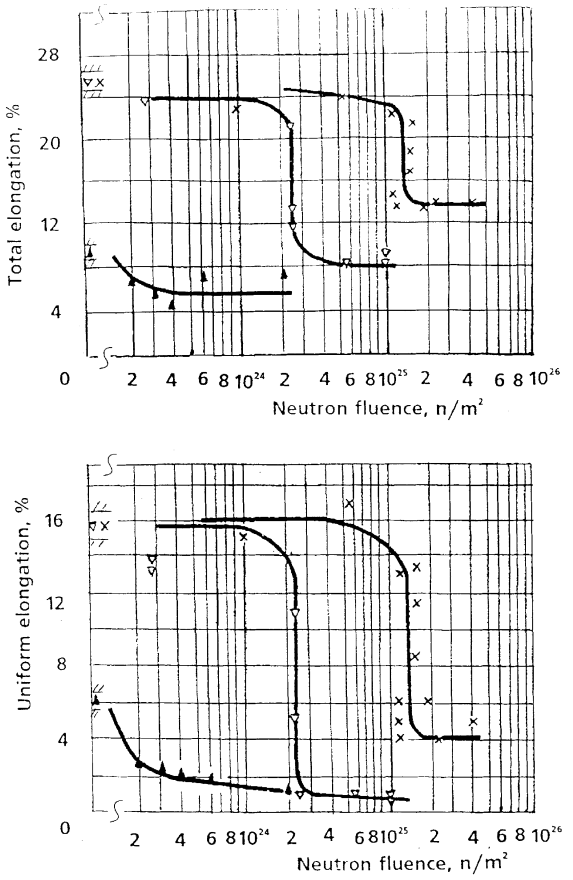

Fig. 2. Total and uniform relative elongation of RK-20 alloy as a function of neutron fluence (E ⩾ 0.5 MeV). Irradiation temperature, °C: ▽ – 250, × – 300, ▲ – 50, Ti–Al–V alloy. $T_{test} = T_{irr}$.

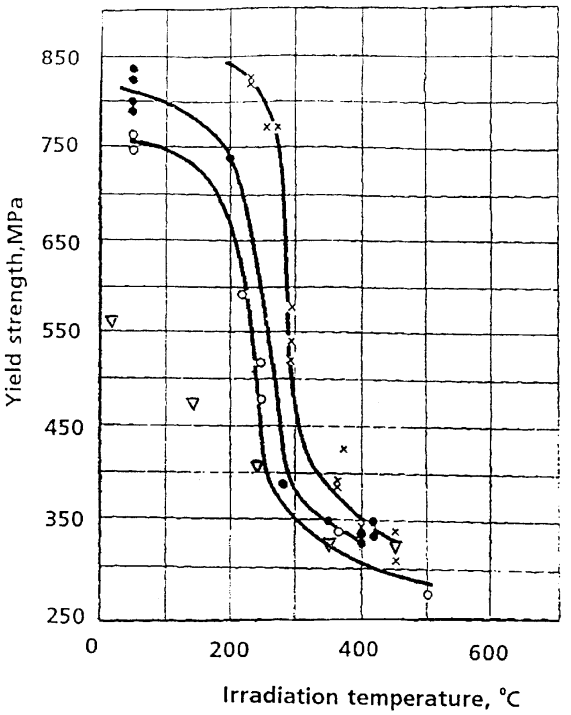

Fig. 3. Yield strength of RK-20 alloy as a function of irradiation temperature. Neutron fluence, n/m^2, (E $\geqslant$ 0.5 MeV): ○ – 2.5×10^{24} n/m^2, ● – 6×10^{24} n/m^2, × – 1.1×10^{25} n/m^2, ▽ – unirradiated. $T_{test} = T_{irr}$.

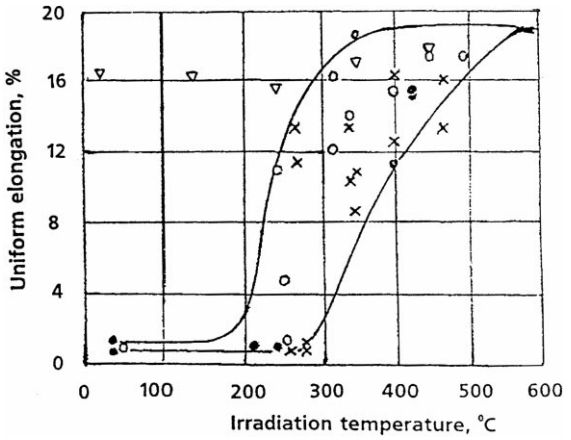

Fig. 4. Uniform elongation of RK-20 alloy as a function of irradiation temperature. Neutron fluence, n/m^2 (E $\geqslant$ 0.5 MeV): ○ – 2.5×10^{24} n/m^2, ● – 6×10^{24} n/m^2, × – 1.1×10^{25} n/m^2, ▽ – unirradiated. $T_{test} = T_{irr}$.

behaviour. The values $\Psi = 67\%$ and $\Psi = 65\%$ have been measured after an irradiation to 4×10^{24} n/m^2 at $T_{irr} = 200 \sim 250$°C and $T_{irr} = 400$°C, respectively. The control (unirradiated) data are $\Psi = 70\%$ for $T_{test} = 200 \sim 250$°C and $\Psi = 75\%$ for $T_{test} = 400$°C.

The threshold type of dose and temperature curves Figs. 1–4 enables us to assume that there exist different mechanisms of irradiation influence in the low temperature (less than 250°C) and in the high temperature (more than 350°C) regions. In order to understand this phenomenon it is necessary to carry out a detailed study of the nature, density and distribution of irradiation defects arising in the alloy after irradiation at $T_{irr} < 250$°C.

It is also necessary to have information about features of the defect structure evolution in the process of plastic deformation up to the stage of critical structure formation which directly precedes the macroscopic fracture, along with the results of fractographic studies. Some of the preliminary results of these studies are presented below.

3.2. Microstructure

The microstructure of the alloy in the initial unirradiated state consists of α-phase plates of 0.2–2 μm width, parallel to each other and grouped in colonies of average size about 30 μm (Fig. 5(a)). The density of the uniformly distributed dislocations does not exceed 5×10^{12} m^{-2}. High angle boundaries of colonies and low angle boundaries of plates are free from any precipitations.

Neutron irradiation at 200 $\sim$ 250°C results in a large quantity (5×10^{23} m^{-3}) of 2–3 nm radiation defects of 'black dots' type, uniformly distributed in the α-plates (Fig. 5(b)). The observed defects do not give additional reflections in diffraction patterns and therefore they cannot be interpreted as radiation-induced precipitation. Most likely, the black dots are clusters of interstitial atoms. It should be noted as well that low temperature irradiation doesn't change the state of boundaries and that they remain free of precipitation.

After neutron irradiation at 400°C, the defect structure of the alloy is different from the structure described above. In the inside volumes of plates the density of the uniformly distributed dislocations increases and dislocation loops of 10–30 nm are formed. The volume density of these loops doesn't exceed 0.5 $\sim$ 1×10^{21} m^{-3} (Fig. 5(c)). At the high-angle boundaries of colonies the precipitates of 0.1–0.2 μm were found (Fig. 5(d)). By means of microdiffraction methods and EDX-analysis, these precipitates were identified as intermetallides Ti-$ZrFe_{0.5}Ni_{0.5}$ having hexagonal lattice of $a = 0.523$ nm, $c = 0.853$ nm parameters.

The formation of narrow long bands (channels) with reduced radiation defect density was found to be typical for the microstructure of the sample strained up to 3.3% after the low temperature irradiation (Fig. 5(e)). The dislocations observed within some of the channels (Fig. 5(f)) were identified as C + A dislocations.

Fig. 6 shows the fracture appearance of the irradiated RK-20 alloy. It is seen that the dimple ductile

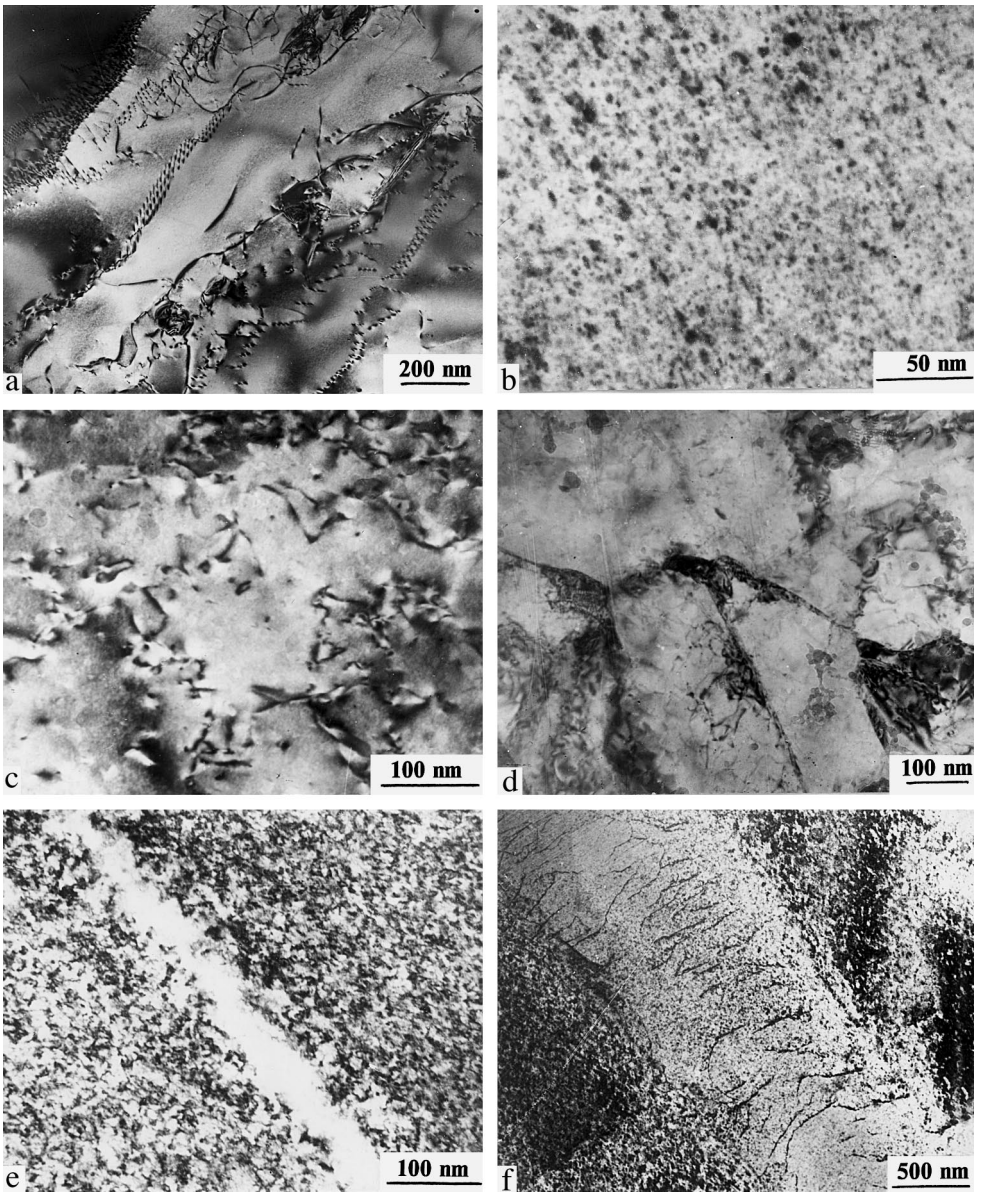

Fig. 5. TEM microstructures of RK-20 alloy: a – unirradiated, b – 4×10^{24} n/m^2, $T_{irr} = 200 \sim 250$°C; c,d – 4×10^{24} n/m^2, $T_{irr} = 400$°C; e,f – 4×10^{24} n/m^2, $T_{irr} = 200 \sim 250$°C; $\varepsilon = 3.3\%$.

transgranular fracture is typical for the examined material after the low temperature irradiation (Fig. 6(a)). Both dimple transgranular fracture and the elements of the ductile intergranular fracture are observed in the material after neutron irradiation at 400°C (Fig. 6(b)).

4. Discussion

The observed microstructural features clearly demonstrate the nature of the sharp difference between the values of irradiation hardening at $T_{irr} < 250$°C and at $T_{irr} > 350$°C. (Fig. 1). It is natural that the observed microstructural differences should in exactly the same way affect the plasticity characteristics because of the change of plastic deformation mechanisms. Deformation of material irradiated at 400°C and characterized by a relatively small density of dislocation loops would proceed in a normal way in the initial stages of plastic flow due to slipping and climbing of single dislocations, which, in a first approximation, are uniformly distributed in a volume. In material irradiated at 200 ~ 250°C,

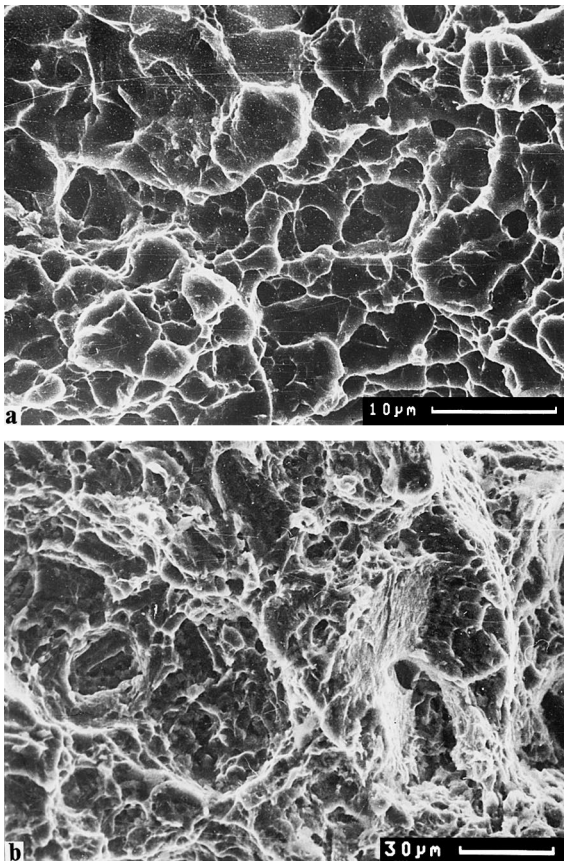

Fig. 6. Fracture appearance of RK-20 alloy irradiated at 200 ~ 250°C (a) and 400°C (b).

where the defect structure consists of a great number of irradiation defects uniformly distributed in a volume and being powerful barriers (pinning points) for moving dislocations, typical channelling of plastic strain is observed. Already at small values (about 0.7%) of plastic strain, localization of plastic flow takes place. In this case the strain is proceeding at mesolevel, concentrating in narrow long channels, practically free of radiation defects, where C + A dislocations move easily (Fig. 5(e) and (f)). As the strain develops, more and more volumes are becoming free of irradiation defects, and further evolution of strained structures proceeds by general laws typical for the high-plastic α-alloys [5]. It is completed by the formation of specific fragmented microstructure in which ductile transcrystalline microcracks are nucleated, grow up and join [6]. Just for this reason, in spite of a sharp reduction of uniform elongation values, the alloy irradiated at low temperature is ruptured after the same local strain, due to the same mechanisms of voids nucleation, growth and coalescence with formation of a typical dimple transcrystalline fracture, what in the initial unirradiated state (Fig. 6(a)).

As to the fracture mechanisms of RK-20 alloy irradiated at 400°C, they are combinations of dimple transcrystalline fracture with the elements of an intergranular one (Fig. 6(b)). The last mentioned is explained by a redistribution of Fe, Ni impurities between the matrix and grain boundaries and by precipitation of intergranular intermetallide phases. The appearance of the intergranular components affects only characteristics of ultimate plasticity. Because of the ductile nature of intergranular fracture and its relatively small contribution, the observed reduction of ultimate plasticity characteristics is quite negligible.

5. Conclusions

Mechanical properties, microstructure and fracture appearance of two titanium α-alloys for fusion application were studied after neutron irradiation to $10^{25} \sim 2.2 \times 10^{26}$ n/m^2 at 50–400°C. The following was observed.

1. The incubation period and the threshold type of dose and temperature curves are characteristic features of titanium alloys radiation behaviour. The incubation fluences of Ti–Zr alloy are higher as compared with that of Ti–Al–V alloy.
2. Ti–Zr alloy demonstrates strong radiation hardening at $T_{irr} \leqslant 250$°C and low hardening at $T_{irr} > 300$°C. High values of total elongation and area reduction as well as ductile fracture appearance are typical for this material at all examined irradiation temperatures.
3. The radiation defects uniformly distributed within the α-plates of Ti–Zr alloy are the black dots at $T_{irr} \leqslant 250$°C and dislocation loops 10–30 nm at $T_{irr} = 400$°C. TiZr(Fe, Ni) grain boundary precipitates are formed during high temperature irradiation.
4. The mechanism of plastic deformation by channel formation is observed in Ti–Zr alloy after the low temperature irradiation.

References

[1] I.V. Altovsky, I.V. Gorynin, O.A. Kozhevnikov et al., Perspectives of usage of titanium α-alloys as structural material of the first wall of low-temperature discharge chamber of fusion reactors, in: Study and Development of Materials for Fission Reactors, Science, Moscow, 1981, pp. 141–146.

[2] V.N. Tebus, E.F. Alekseev, I.V. Golikov, Influence of reactor irradiation and helium-3 on mechanical properties of alpha-titanium alloys, Fizika metallov i metallovedenie, N. 5, 1990, pp. 160–164.

[3] I.V. Gorynin, V.F. Vinokurov, O.A. Kozhevnikov et al., Radiation resistance of titanium–zirconium based alloy as structural material used in nuclear power engineering, Material Science Problems, 1, North-West Materials Research Society, 1995, pp. 54–60.

[4] I.V. Gorynin, V.F. Vinokurov, O.A. Kozhevnikov, V.V. Rybin, I.I. Yarmolovich, Plasma Devices Operations 4 (1995) 1.
[5] I.V. Gorynin, E.V. Nesterova, V.V. Rybin, Crystallographic and morphological features of the imperfect structural evolution in plastically deformed alpha titanium, Sixth World Conference on Titanium, 1988, vol. 1, pp. 124–127.
[6] V.V. Rybin, Large Plastic Deformation and Fracture of Metals, Metallurgiya, Moscow, 1986, p. 224.